Nucleic Acids Research, 1993, Vol. 21, No. 21 4975–4980

DNA methylation by N-methyl-N-nitrosourea: methylation pattern changes in single- and double-stranded DNA, and in DNA with mismatched or bulged guanines

Richard L.Wurdeman, Michelle C.Douskey and Barry Gold*
Eppley Institute for Research in Cancer and Allied Diseases and Department of Pharmaceutical Sciences, University of Nebraska Medical Center, Omaha, NE 68198-6805, USA

Received May 4, 1993; Revised and Accepted September 14, 1993

ABSTRACT

The detection of abnormal DNA base pairing arrangements and conformations is chemically probed in synthetic ^{32}P-end-labeled deoxyribonucleotide oligomers using N-methyl-N-nitrosourea (MNU) and 2,12,-dimethyl-3,7,11,17-tetraazabicyclo-[11.3.1]hept-adeca-1-[17],2,11,13,15 pentaene-Ni (II) (Ni-complex) with $KHSO_5$. The DNA targets studied are single-stranded (s-s) DNA, double-stranded (d-s) DNA, d-s DNA with G-G, G-A and G-T mismatches, d-s DNA with a single bulged G and d-s DNA with two bulged G's. The effect of the non-Watson – Crick structures on the formation of N7-methylguanine (N7-MeG) by MNU and the oxidation of G by Ni-complex is reported along with the T_m's and circular dichroism spectra of the different duplex oligomers. The results for MNU and Ni-complex show that the qualitative and quantitative character of the cleavage patterns at a G_3 run change with the nature of the abnormal base pairing motif. Based on the DNA substrates studied, the results indicate that a combination of reagents which report electronic and steric perturbations can be a useful approach to monitor DNA mismatches and bulges.

INTRODUCTION

The development of chemical reagents to probe DNA conformations in solution is of ongoing interest since spectroscopic techniques are either limited by the information that they provide or by the size of the structures that can be studied. Current approaches to investigate DNA structures and conformations involving G depend on differences in the accessibility of the N7-G position which reflect either changes in the dimensions of the major groove or the positioning of the N7-G atom in the helix. Accordingly, the reactivity of N7-G with these reagents is generally lowest in Watson–Crick d-s DNA, higher in non-standard duplexes and highest in s-s DNA. In order to develop additional methods to characterize the conformational environment around guanine residues based on non-steric factors, the reactions of MNU with DNA's containing a variety of non-Watson–Crick base pairing arrangements was studied. MNU reacts with DNA predominantly at the N7-G position (~65% yield) (1), and shows sequence-dependent reactivity (2–4). The sequence selectivity of MNU and related alkylating agents is thought to be due to changes in the electrostatic potential of the N7-G position as a consequence of the nature of flanking bases (2–8). To complement the MNU reactions, the oxidative cleavage of the same DNA oligomers by 2,12,-dimethyl-3,7,11,17-tetraazabicyclo-[11.3.1]heptadeca-1-[17], 2,11,13,15 pentaene-Ni(II) (Ni-complex) in the presence of $KHSO_5$ (9,10) was analyzed. The Ni-complex is sensitive to the steric accessibility of N7-G and has been previously used to probe mismatches, bulges and loop structures in oligomers (10). The specific targets employed in this study contain a central $(G)_3$ run and are single-stranded (s-s) DNA (1), double-stranded (d-s) DNA (1+2), d-s DNA in which a G residue is mismatched with either G (1+3), A (1+4), or T (1+5), and d-s DNA with a single (1+6) or double (1+7) G bulge site. The effect of temperature on the sequence specificity for the methylation of 1 and 1+2 is also reported along with the UV determined T_m's and the circular dichroism (CD) spectra for each duplex.

1 = 5′-d(CACTG^{5}G^{6}G^{7}ACTG^{11}C)
2 = 3′-d(GTGACCCTGACG) 3 = 3′-d(GTGACGCTGACG)
4 = 3′-d(GTGACACTGACG) 5 = 3′-d(GTGACTCTGACG)
6 = 3′-d(GTGACCTGACG) 7 = 3′-d(GTGACTGACG)

METHODS

Preparation of oligomers

Oligomers 1–7 were prepared on a DNA synthesizer (Applied Biosystems Inc.) using standard phosphoramidite chemistry and the crude oligomers purified by high pressure liquid chromatography (HPLC) using a C8 reverse phase column. Oligomer 1 was 5′-[^{32}P]-end-labeled with T4 kinase (BRL) in the presence of γ-^{32}P-ATP (Amersham) and then purified by electrophoresis on a 2% polyacrylamide gel (11). In the reactions

* To whom correspondence should be addressed

with d-s DNA, the two strands were combined and heated to 80°C in a large water bath which was allowed to slowly cool to room temperature overnight.

Reaction of DNA with MNU

The 5′-[^{32}P]-end-labeled 1 (with or without 2−7) was incubated with 500 μM MNU (Aldrich) in 10 mM *tris*(hydroxymethyl)aminomethane (Tris)-HCl buffer (pH 7.8) containing 100 mM NaCl and 1 mM ethylenediaminetetraacetic acid (EDTA) for 2 h at 20°C. These conditions provide less than 1 cleavage per strand even at the elevated temperatures (see below). The reactions were terminated by cooling in ice and precipitation of the DNA with NaOAc/EtOH followed by repeated washing with cold EtOH.

Ni-complex reaction

The reaction of the DNA with 3 μM Ni-complex and 60 μM $KHSO_5$ was carried out at pH 7.0 in 10 mM K phosphate or Tris−HCl buffer (data not shown) containing 100 mM NaCl as previously described (10), with the following exceptions. The DNA was not dialyzed prior to piperidine treatment and the piperidine concentration used to generate strand breaks (see below) was 1 M. If the dialysis step is included, strand breaks can be effected by 0.2 M piperidine (10). As with MNU, the conditions used resulted in <1 cleavage per strand.

Generation of strand breaks

The DNA, after drying *in vacuo*, was treated with 1 M piperidine for 20 min at 90°C to selectively convert the G lesions into strand breaks (11). After removal of the piperidine *in vacuo*, the DNA was suspended in loading buffer (80% deionized formamide, 50 mM Tris-borate, pH 8.3, 1 mM EDTA) containing no dye markers and denatured by heating at 90°C for 1 min and cooling in ice. The DNA was placed into wells on top of a 20% polyacrylamide (7.8 M urea) denaturing gel and the gel run at 75 W (~55°C). The standard Maxam-Gilbert G and G+A reaction lanes were included as sequence markers (11). Control lane DNA received the same treatment except it was not incubated with MNU or Ni-complex. The gel was then exposed to Kodak X-OMAT AR film at −70°C and the resulting autoradiogram analyzed using a Shimadzu CS-9000 scanning densitometer. In some cases the bands were excised from the gels and the quantitation performed by scintillation counting. Both densitometry and scintillation gave the same results and only densitometry data are presented (Figs. 1 and 2).

Temperature effects

The reactions of 1 and 1+2 with 500 μM MNU were performed as described above except that the temperature of the incubations was varied as indicated in the legend for Fig. 3, which provides the autoradiogram of the results. The control lane contains DNA exposed to the 80°C temperature.

Thermal stability

The denaturation of 1+2−7 as a function of temperature in the same 10 mM Tris buffer with 100 mM NaCl and 1 mM EDTA was followed by monitoring their UV absorbance at 260 nm (Table 1). T_m's were calculated by plotting $d(A_{260})/dT$ vs T.

CD measurements

The CD spectra of 1+2−7 (189 μM) were obtained at 20°C on a Jasco 600 CD spectrophotometer in 10 mM Tris−HCl buffer (pH 7.8) containing 100 mM NaCl. The spectra shown are an average of 15 scans (Fig. 4). Using the same conditions, the CD spectrum of 1 was also run over a range of temperatures from 25°C to 75°C at 10°C intervals (Fig. 5).

RESULTS

The autoradiogram of the sequencing gel and the uncorrected densitometric analyses of the G5-7 cleavage bands generated by MNU with 5′-^{32}P-1 at 20°C in 100 mM NaCl in the absence and presence of 2−7 show that the nature of the base pairing arrangement near the G_3 run affects the cleavage pattern (Fig. 1). The G-cleavage profile at the $(G)_3$ run in 1+2−7 in the presence of 0 or 200 mM NaCl is qualitatively identical with that observed at 100 mM NaCl, except there is a quantitative decrease in methylation with increasing salt concentration (data not shown). The Ni-complex + $KHSO_5$ induced fragmentations of the different DNA's also show a sensitivity to strandedness and base pairing motif (Fig. 2).

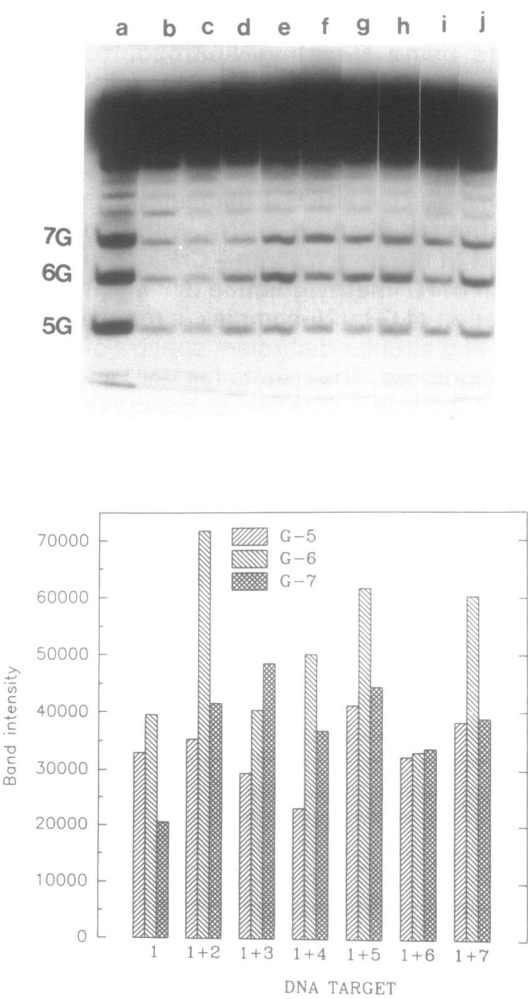

Figure 1. (**top**) MNU-mediated cleavage of 1, 1+2 and 1+3−7: lane a, G-lane; lane b, G+A lane; lane c, control; lanes d−f, DNA treated with 500 μM MNU at 20°C; lane d, s-s DNA 1; lane e, 1+2; lane f, 1+3; lane g, 1+4; lane h, 1+5; lane i, 1+6; and lane j, 1+7. (**bottom**) Uncorrected densitometry: lanes d−j.

In terms of the densitometry results (Figs. 1 and 2), repetitive scans of the same lane can be reproduced to ± 1−2%. Comparison of experiments where the amount of DNA, which is not limiting, was increased showed that the relative percentages of bands within a given lane (that is the ratio of G5:G6:G7) ranged from ± 0−8%, with an average variation of 3% (data not shown). This means that the qualitative methylation pattern for a given target is very reproducible. In the same experiments in which the DNA concentration was changed, differences of 0−15% are seen with the same target DNA when comparing the absolute intensities of specific G's from different lanes. The variations in the absolute intensities are attributed to errors in delivering the exact MNU concentration to each incubation and the amount of ^{32}P-labeled DNA loaded onto each lane.

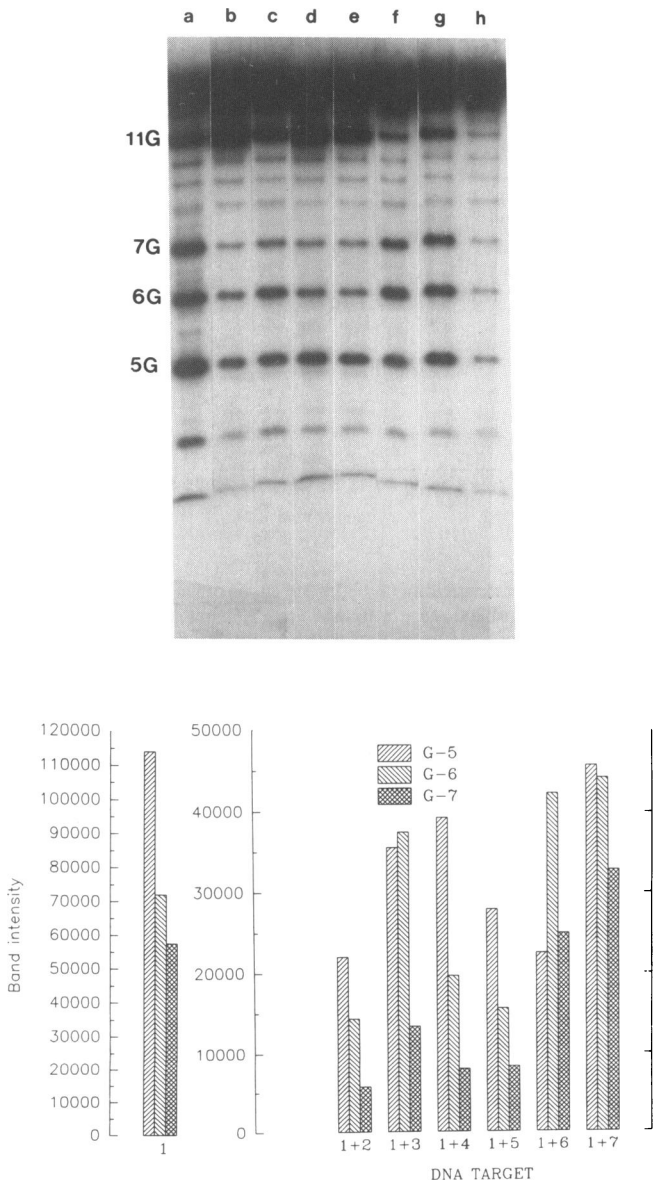

Figure 2. (**top**) Ni-complex + $KHSO_5$ fragmentation of 1, 1+2 and 1+3−7: lanes a−g, DNA treated with 500 μM Ni-complex + $KHSO_5$ at 0°C; lane a, s-s DNA 1; lane b, 1+2; lane c, 1+3; lane d, 1+4; lane e, 1+5; lane f, 1+6; and lane g, 1+7; lane h, control. (**bottom**) Uncorrected densitometry: lanes a−g.

The band that appears near the top of each lane just below the band that corresponds to the full length oligomer is attributed to G11 (Fig. 1). The intensity of this band does not respond to changes in temperature (Fig. 3), MNU concentration (data not shown), or salt concentration (data not shown). A similar fluctuation is also seen with the Ni-complex reagent (Fig. 2). It is possible that the abnormal behavior of G11 is due to its position once removed from the terminal base.

The results with MNU demonstrate that there is a distinct N7-MeG pattern for 1 at 20°C with the ratio of G5-7 being 1.6:1.9:1.0 relative to d-s target 1+2 where the ratio is 1.0:2.1:1.2 (Fig. 1). The overall methylation at N7-G within the $(G)_3$ run in 1 (Fig. 1) or with 1+2 at temperatures >60°C (Fig. 3) is reduced by ~40% as compared to 1+2 at 20°C. Duplex 1+2 has a T_m of 56°C (Table 1). Qualitatively, the N7-MeG pattern at the G5-7 run varies with the type of mismatch and differences in the absolute intensities occur at the central G6 as well as at the flanking G residues. In the duplex with the single bulge site (1+6), the intensities of G5-7 are very similar to each other and differ by approximately +10, −50 and −20%, respectively, relative to 1+2, with an overall decrease at the G_3 run of 30%. The addition of the second bulge (1+7) increases the cleavage at G6 and in comparison to 1+2, G5-7 are changed by approximately +10, −15 and −5%, respectively, with an overall decrease at the G_3 run of 10%.

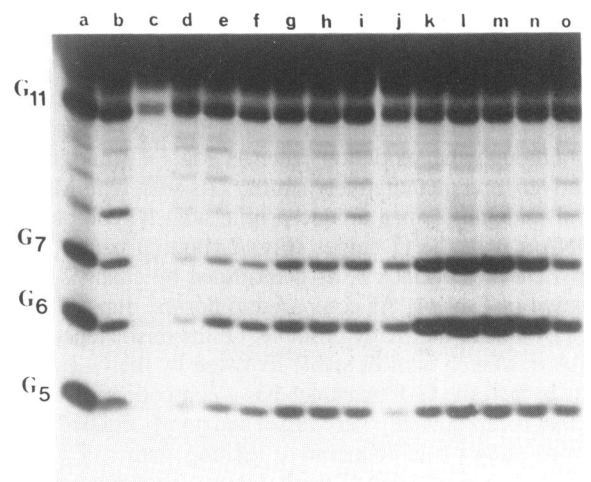

Figure 3. MNU-mediated DNA cleavage of 1 and 1+2 as a function of temperature: lane a, G-lane; lane b, G+A lane; lane c, control; lanes d−i, s-s DNA 1 treated with 500 μM MNU at 0, 20, 40, 50, 60 and 80°C, respectively; lanes j−o, d-s DNA 1+2 treated with 500 μM MNU at 0, 20, 40, 50, 60 and 80°C, respectively.

Table 1. Melting temperatures for duplex DNA oligomers[a]

DNA	description	T_m (°C)	ΔT
1+2	normal	56	–
1+3	G-G mismatch	44	12
1+4	G-A mismatch	51	5
1+5	G-T mismatch	46	10
1+6	single G bulge	43	13
1+7	double G bulge	31	25

[a] See Methods section for experimental details.

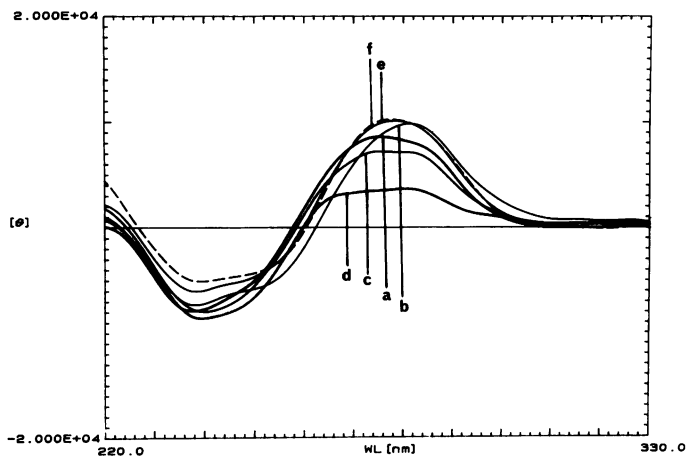

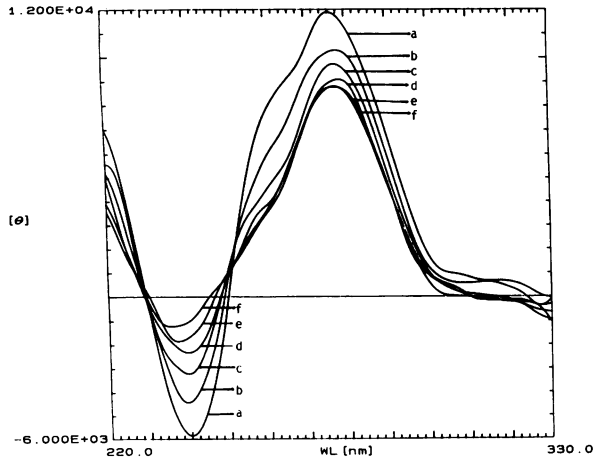

Figure 4. CD spectra of 189 μM 1+2−7 in 10 mM Tris−HCl buffer (pH 7.8) containing 100 mM NaCl at 20°C: a, 1+2; b, 1+3; c, 1+4; d, 1+5; e, 1+6 (dashed line); and f, 1+7 (solid line).

The MNU-induced fragmentation of 1 and 1+2 as a function of temperature appears in Fig. 3. There is a general increase in the overall level of methylation as the reaction temperature is elevated to 40°C. It is assumed that this increase results from more extensive hydrolysis of MNU into reactive intermediate at the elevated temperatures. As noted above, at 60°C, which is above the T_m of 1+2, the methylation decreases.

The reaction with Ni-complex shows that s-s DNA reacts > 5-fold better than does d-s DNA 1+2 and at least 2.5-fold better than 1+3, the best of the mismatched targets (Fig. 2). All of the targets are more efficiently degraded by Ni-complex than 1+2, although the oxidation patterns for 1+2 and 1+5 are qualitatively and quantitatively similar. As seen with MNU, the G-G mismatch affords a unique profile with Ni-complex as do the DNA's with the G bulges (Fig. 2, bottom panel).

The T_m's of the DNA's, as determined by changes in A_{260}, are shown in Table 1. As compared to normal duplex 1+2, all of the DNA's are thermally unstable. Of the mismatched DNA's the G-A mismatch is most stable followed by the G-T and G-G motifs. In fact, the G-T mismatch has a non-cooperative melting curve that is reproducibly very broad and poorly defined. Duplex 1+6 also shows non-cooperative melting with a T_m roughly 15°C lower than of 1+2. The s-s DNA 1 shows no change in its A_{260} or λ_{max} with increasing temperature and the duplex with the double bulge site (1+7) has a poorly defined melting curve with a T_m estimated to be 31°C.

The CD spectra of the d-s DNA oligomers are shown in Fig. 4. The d-s DNA's exhibit B-form CD spectra with the intensities of the long and short wavelength bands varying with structure. The effect of temperature on the CD of 1 appears in Fig. 5. The results show that there is a decrease in the magnitude of the long wavelength band and a small red shift of the λ_{max} for 1 up to 65°C with isoelliptic points at 229 and 249 nm that coincide with the intersection line [Θ = 0].

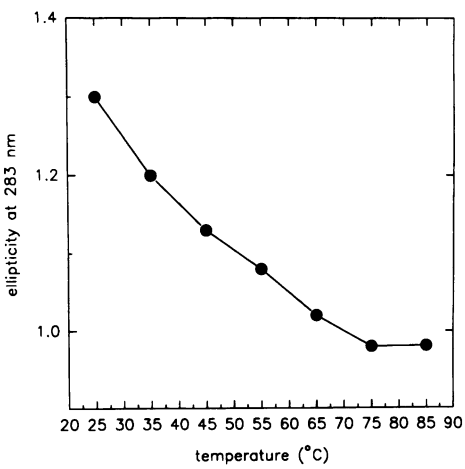

Figure 5. Effect of temperature (a−f: 25, 35, 45, 55, 65 and 75°C, respectively) on the CD spectra of 200 μM 1 in 10 mM Tris−HCl buffer (pH 7.8) containing 100 mM NaCl (**top**) and the plot of the change in the molar ellipticity of the 283 nm band with temperature (**bottom**).

DISCUSSION

Both MNU and Ni-complex initiate strand scission through electrophilic interaction with N7-G; however, the similarity between the two reagents ends there. The formation of N7-MeG by MNU is sensitive to DNA sequence with the difference between the strongest and the weakest methylation sites in restriction fragments being almost 10-fold (3,4). It has been proposed that the origin of the sequence selectivity for the reaction of MNU with d-s DNA is related to variations in the electrostatic potential at different N7-G centers (2−8). In contrast to MNU, the relative reactivity of Ni-complex mediated oxidation of G is thought to be most dependent on the accessibility of the reagent to the N7-G major groove site (10). The difference in the mechanisms of DNA recognition by the two reagents is evident from their sequence selective modification of the varied DNA targets; MNU and Ni-complex never afford the same cleavage pattern (Figs. 1 and 2). Despite the differences in the mechanism of backbone cleavage, both compounds, albeit in their own way, can distinguish between Watson−Crick and 'unnatural' base pairing motifs. It should be noted that dimethyl sulfate shows no sequence selectivity in its reactions with 1+2 (Fig. 1, lane a). Therefore, it is possible that the preferential oxidation of certain G's in 1+2 by the Ni-complex is not solely based on steric effects.

Mismatched DNA

Overall, the G-A mismatch affects methylation and oxidation at the 5'-residue more than at the mismatch. This is unexpected since it would have been predicted that G7 would be most responsive to the introduction of the mismatch based on the observation that the MNU-mediated formation of N7-MeG is most sensitive to the nature of the 5'-base (3,4). We would argue that the relationship between G6 and G7 in 1+4 is very similar to that in 1+2 and that the mismatch causes a disruption 5' of the mismatch on the G rich strand. The results with Ni-complex are congruous with this interpretation. The crystal structure of $d(CGCAAGCTGGCG)_2$ provides evidence that a G-A mismatch can result in the virtual loss of intrastrand stacking between the G in the mismatch and the 5'-residue. (12). Obviously, the stacking of bases is dependent on many helical features that can affect the planar orientation of the flanking bases relative to one another, i.e. base tilt, propeller twist, roll, etc. The bases in the G-A mismatch can make two H-bonds via three distinct base pairing motifs: G_{anti}-A_{anti}, G_{anti}-A_{syn}, and G_{syn}-A^+_{anti} (12−18). In the former two arrangements the N7-G site is open for methylation and oxidation. In the G_{syn}-A^+_{anti} motif, that has only been observed at lower pH (17,18), the N7-G site is blocked by Hoogsteen pairing with the protonated imino tautomer of A. The persistence of methylation and oxidation at N7-G in 1+4 is additional evidence that in solution the G_{syn}-A^+_{anti} arrangement does not exist near neutrality. It is of interest that the G-A mismatch which has the highest T_m and methylation and oxidation patterns qualitatively similar to normal duplex 1+2, also has the highest frequency of any mismatch in escaping detection by DNA mismatch repair enzymes (19,20).

The G-T mismatch may be important in the formation of 'spontaneous' mutations at CpG dinucleotide repeats due to the deamination of 5-methylcytosine (21). It has been established from NMR studies that G-T forms two H-bonds via a Wobble base pair (22−24). Duplex 1+5 has a low T_m with non-cooperative melting that is consistent with extensive disruption of the double helix (25). Despite the thermal instability of 1+5, the change in its reaction with Ni-complex relative to 1+2 is small; there is less than a 20% overall increase in cleavage at G5-7 and the pattern is almost identical to 1+2. The methylation pattern is also very close to that of 1+2, the only difference being a 15% reduction in cleavage at the mismatched G6. This small change in the methylation pattern parallels the maintenance of normal intrastrand stacking of the mismatched G that has been found in the crystal structure of $d(CGCGAATTTGCG)_2$ (22). Some disruption of stacking relative to the normal dodecamer is observed in the complement strand. The results for 1+5 demonstrate that a major change in thermal stability does not necessarily cause concomitant stereo or electronic changes in the duplex as measured by the two reagents. Another observation is that the G-T mismatch and 1+2 have comparable CD spectra. However, over interpretation of the CD is dangerous, since the CD spectra of the single- and double-G bulge DNA's 1+6 and 1+7 are almost superimposable (Fig. 4) while the methylation and oxidative patterns are quite dissimilar. A final note on the G-T mismatch is that it is the mismatch most rapidly repaired by bacterial methyl-dependent mismatch repair enzymes (20).

The G-G mismatch results in obvious aberrations in both the methylation and oxidation reactions. Duplex 1+3 is unique in that the 3'-G becomes the most pronounced methylation site due to a combined 40% reduction at G6 and a 15% increase at G7. In studying the MNU methylation patterns in several large restriction fragments and synthetic oligomers, we have never observed a similar result in a G_3 sequence (3,4, unpublished results). The reaction of Ni-complex with 1+3 is also different than that seen with all the other oligomers, and is consistent with a general increase in the accessibility of all the G's with the greatest impact being at G6 and G7. NMR and crystallographic assignments of the structures of DNA with G-G mismatches include G_{anti}-G_{syn} (26,27), G_{anti}-inosine$_{syn}$ (28) and G_{anti}-G_{anti} (29) pairing arrangements. The G_{anti}-G_{syn} alignment affords two H-bonds but requires significant displacement of one of the mismatched G's into the major groove. The G_{anti}-G_{anti} model contains a poorly H-bonded G-G pair with the bases bulged out of the helix and poorly stacked with the flanking bases on both strands (29). Since the N7-position in a G_{syn} of a G_{anti}-G_{syn} pair is H-bonded to the N^2 amino group of the G_{anti} base, the persistence of G6 methylation and oxidation in 1+3 suggests that G6 is not a *syn* base. However, it is possible that G6 in 1+3 exists as a dynamic mixture of *syn* and *anti* alignments. Certainly, the structure of the G-G mismatch, as well as any other mismatch, will be dependent on the nature of the flanking bases. The rate of bacterial repair of the G-G mismatch is slightly less than that of the G-T analogue (20) which suggests that the noted distortions detected by MNU and Ni-complex do not relate in any simple way to the recognition of mismatches by the bacterial DNA mismatch repair enzyme system.

Bulged DNA

The results with MNU and Ni-complex show that both compounds can distinguish between 1+2, 1+6 and 1+7. The methylation of the duplex with a single G bulge shows that G5-7 are equal targets for the methanediazonium ion while the addition of a second unpaired G affords a pattern more similar to 1+2 and almost identical to the G-T mismatch 1+5. Reduced reaction (~50%) at G6 is the predominant difference between the pattern for 1+6 and 1+2. It was unexpected to find in 1+7 that the lack of two cytidylic acid residues in the complement strand does not alter the CD spectra or diminish the extent of methylation relative to that of the single G bulge. The Ni-complex reagent shows an overall 2-fold enhanced oxidation in 1+6 relative to 1+2, with the major increase being localized at G6 and G7, a result consistent with the unpairing of these bases as a consequence of the bulge. In 1+7 there is a 3-fold increase in cleavage by Ni-complex and all three G's show almost the same reactivity due to rapid migration of the bulge throughout the G_3 sequence. Despite the increased reactivities of the G's in 1+7 with Ni-complex, the combined intensities of the bands are only 50% of that observed in s-s DNA. A study on a G bulge in a G_3-C_2 region of an oligomeric DNA using NMR and energy minimization suggests that the central G spends more time without a complement than the flanking G's (30). The picture provided by MNU with 1+6 is in general agreement with this description as methylation of the central G is most affected. The Ni-complex shows that the predominant location of the bulge in the middle of the G run in 1+6 also results in substantial opening of the groove at G7, although the access to N7-G is still limited relative to s-s DNA.

Single-stranded DNA

It is apparent from the current work that s-s DNA is a poorer target for MNU than d-s DNA. A preference of N-methyl-

N'-nitro-N-nitrosoguanidine (MNNG) for d-s DNA has previously been described using HPLC analysis of the adduct products from digested DNA (31,32). The resemblance between MNNG and MNU results is not surprising since both compounds hydrolyze to afford the same methanediazonium ion, the ultimate DNA methylating species (4). The decrease in alkylation of s-s DNA may result from: (i) the exposure of other competitive nucleophilic sites (e.g. N3-C, N1-A, etc.) that are normally sterically blocked or electronically deactivated because of Watson–Crick H-bonding; or (ii) a change in reactivity due to a modification in base stacking. Since the methylation of DNA by dimethyl sulfate, the S_N2 alkylating agent used to generate the Maxam–Gilbert G-lane, is not affected by DNA strandedness (data not shown), the former argument is not an attractive explanation of the data.

The generation of a distinct MNU cleavage pattern with 1 implies that the s-s oligomer exists in a conformation distinct from 1+2, at least at the $(G)_3$ run, and is not in a random coil. The reaction of 1 with Ni-complex also shows that accessibility of the N7-G sites in s-s DNA is not uniform with G5 being a 2-fold better substrate than G7. The CD spectra at different temperatures (Fig. 5) verifies the persistence of ordered base helicity in 1, a phenomenon that has been previously reported for other s-s DNA's (33). The change in the methylation pattern of 1 as function of temperature does not occur until the reaction temperature exceeds 60°C (Fig. 3, lane h). In contrast, the loss of helicity of the bases with increasing temperature continues through 65°C (Fig. 5, bottom panel) and the observation of isoelliptic points signify that 1 exists as a mixture of two distinct structural states. It is possible that the observed lack of correlation between the CD (Fig. 5) and methylation (Fig. 3) data is because the G_3 run is the last region to adopt a random coil as the temperature is increased; therefore, changes in the CD spectrum below 60°C may not reflect any significant change in the helical state of the G_3 stretch. The significant temperature related decrease in the CD of 1 (30%) with little concomitant change in the UV spectrum implies that there is weak base interaction in the s-s structure, even at low temperature. As postulated above, this reduction in stacking of the G run results in a decrease in the electrostatic potential at this sequence (5), which in turn would explain the decrease in the reaction with MNU.

In conclusion, we have shown that the methylation pattern induced by MNU in a G_3 run can distinguish between normal and abnormal DNA structures; the type and degree of change in the pattern is related to the nature of the structure. Accordingly, MNU, which is sensitive to electronic and not steric factors, in conjunction with other reagents that basically report the accessibility of N7-G, e.g. Ni-complex, may be useful in the monitoring the formation and repair of mismatches, bulges and other non-Watson–Crick base pairs in large DNA fragments. However, the general utility of MNU to detect unusual base pairing arrangements at G will require further evaluation in a wide variety of targets. Finally, there appears to be no relationship between the reaction preferences of MNU or Ni-complex with the previously reported rates of mismatch repair by DNA repair enzymes.

ACKNOWLEDGEMENTS

This work was supported by Grant CA29088 and Laboratory Cancer Grant CA36727 from the National Cancer Institute, and American Cancer Center Core Grant SIG-16. M.C.K. was supported by a summer fellowship from Eli Lilly and Co. We are most grateful to Drs Cynthia Burrows and Steven Rokita for their gift of the 2,12,-dimethyl-3,7,11,17-tetraazabicyclo-[11.3.1]heptadeca-1-[17],2,11,13,15 pentaene-Ni(II) complex.

REFERENCES

1. Beranek, D.T., Weis, C.C. and Swenson, D.H. (1980) *Carcinogenesis*, **1**, 595–605.
2. Briscoe, W.T. and Cotter, L.-E. (1985) *Chem. Biol. Interact.*, **56**, 321–331.
3. Wurdeman, R.L. and Gold, B. (1988) *Chem. Res. Toxicol.*, **1**, 146–147.
4. Wurdeman, R.L., Church, K.M. and Gold, B. (1989) *J. Am. Chem. Soc.*, **111**, 6408–6412.
5. Pullman, A. and Pullman, B. (1981) *Q. Rev. Biophys.*, **14**, 289–380.
6. Hartley, J.A, Gibson, N.W., Kohn, K.W. and Mattes, W.B. (1986) *Cancer Res.*, **46**, 1943–1947.
7. Kohn, K.W., Hartley, J.A., and Mattes, W.B. (1987) *Nucl. Acids Res.*, **15**, 10531–10549.
8. Hartley, J.A, Mattes, W.B., Vaughan, K. and Gibson, N.W. (1988) *Carcinogenesis*, **9**, 669–674.
9. Chen X., Burrows, C.J. and Rokita, S.E. (1991) *J. Am. Chem. Soc.*, **113**, 5884–5886.
10. Chen X., Burrows, C.J. and Rokita, S.E. (1992) *J. Am. Chem. Soc.*, **114**, 322–325.
11. Maxam, A.M. and Gilbert, W. (1980) *Methods Enzymol.*, **65**, 499–560.
12. Webster, G.D., Sanderson, M.R., Skelly, J.V., Neidle, S., Swann, P.F., Li, B.F. and Tickle, I. J. (1990) *Proc. Natl. Acad. Sci. USA*, **87**, 6693–6697.
13. Brown, T., Hunter, W.N., Kneale, G. and Kennard, O. (1986) *Proc. Natl. Acad. Sci. USA*, **83**, 2402–2406.
14. Privé G.G., Heinemann, U., Chandrasegran, S., Kan, L.-S., Kopka, M.L. and Dickerson, R.E. (1987) *Science*, **238**, 498–504.
15. Lane, A.N., Jenkins, T.C., Brown, D.J.S. and Brown, T. (1991) *Biochem. J.*, **279**, 269–281.
16. Carbonnaux, C., Fazakerley, G.V. and Sowers, L.C. (1990) *Nucleic Acids Res.*, **18**, 4075–4081.
17. Brown, T., Leonard, G.A., Booth, E.D. and Kneale, G. (1990) *J. Mol. Biol.*, **212**, 437–440.
18. Carbonnaux, C., van der Marel, G.A., van Boom, J.H., Cognet, J.A.H., Gabarro-Arpa, J., Le Bret, M., van der Marel, G.A., van Boom, J.H. and Fazakerley, G.V. (1991) *Nucleic Acids Res.*, **19**, 6771–6779.
19. Fersht, A.R., Knill-Jones, J.W. and Tsui, W.C. (1982) *J. Mol. Biol.*, **156**, 37–51.
20. Su, S.-S., Lahue, R.S., Au, K.G. and Modrich, P. (1988) *J. Biol. Chem.*, **263**, 6829–6835.
21. Radman, M. and Wagner, R. (1984) *Curr. Topics Microbiol. Immunol.*, **108**, 23–28.
22. Hunter, W.N., Brown, T., Kneale, G., Anand, N.N., Rabinovich, D. and Kennard, O. (1987) *J. Biol. Chem.*, **262**, 9962–9970.
23. Quignard, E., Fazakerley, van der Marel, G., van Boom, J.H. and Guschlbauer, W. (1987) *Nucleic Acids Res.*, **15**, 3397–3409.
24. Kalnick, M.W., Kouchakdjian, M., Li, B.F.L., Swann, P.F. and Patel, D.J. (1988) *Biochemistry*, **27**, 108–115.
25. Moe, J.G. and Russu, I.M. (1992) *Biochemistry*, **31**, 8421–8428.
26. Cognet, J.A.H., Gabarro-Arpa, J, LeBret, M., van der Marel, G.A., van Boom, J.H. and Fazakerley, G.V. (1991) *Nucleic Acids Res.*, **19**, 6771–6779.
27. Skelly, J.V., Edwards, K.J., Jenkins, T.C. and Neidle, S. (1993) *Proc. Natl. Acad. Sci. USA*, **90**, 804–808.
28. Oda, Y., Uesugi, S., Ikehara, M., Kawase, Y. and Ohtsuka, E. (1992) *Nucleic Acids Res.* **19**, 5263–5267.
29. Borden, K.L.B., Jenkins, T.C., Skelly, J.V., Brown, T. and Lane, A.N. (1992) *Biochemistry*, **31**, 5411–5422.
30. Woodson, S.A. and Crothers, D.M. (1988) *Biochemistry*, **27**, 436–445.
31. Singer, B. and Fraenkel-Conrat, H. (1969) *Biochemistry*, **8**, 3260–3266.
32. Bodell, W.J. and Singer, B. (1979) *Biochemistry* **18**, 2860–2863.
33. Gray, D.M., Ratliff, R.L. and Vaughan, M.R. (1992) *Methods Enzymol.*, **211**, 389–406.